Retention of α-pinene oxidation products and nitro-aromatic compounds during riming

Christine Borchers[1], Jackson Seymore[2], Martanda Gautam[2], Konstantin Dörholt[3], Yannik Müller[1], Andreas Arndt[2], Laura Gömmer[2], Florian Ungeheuer[3], Miklós Szakáll[2], Stephan Borrmann[2,4], Alexander Theis[4], Alexander L. Vogel[3], Thorsten Hoffmann[1]

[1]Departmet of Chemistry, Johannes Gutenberg University, Mainz, Germany
[2]Institute for Atmospheric Physics, Johannes Gutenberg University, Mainz, Germany
[3]Institute for Atmospheric and Environmental Sciences, Goethe-University Frankfurt/Main, Germany
[4]Particle Chemistry Department, Max Planck Institute for Chemistry, Mainz, Germany

Correspondence to: Thorsten Hoffmann (t.hoffmann@uni-mainz.de)

Abstract

Riming is an important growth process of graupel and hailstones in mixed-phase zones of clouds, during which supercooled liquid droplets freeze on the surface of ice particles by contact. Compounds dissolved in the supercooled cloud droplets can remain in the ice or be released to the gas phase during freezing, which might play an important role in the vertical redistribution of these compounds in the atmosphere by convective cloud processes. This is important for estimating the availability of these compounds in the upper troposphere, where organic matter can promote new particle formation and growth. The amount of organics remaining in the ice phase can be described by the retention coefficient. Experiments were performed in the Mainz vertical wind tunnel under dry and wet growth conditions (temperature from -12 to -3 °C and a liquid water contents (LWC) of $0.9 \pm 0.2 \ \mathrm{g \ m^{-3}}$ and $2.2 \pm 0.2 \ \mathrm{g \ m^{-3}}$) as well as different pH values (4 and 5.6) to obtain the retention coefficients of α-pinene oxidation products and nitro-aromatic compounds. For cis-pinic acid, cis-pinonic acid, and $(-)$-pinanediol mean retention coefficients of 0.96 ± 0.07, 0.92 ± 0.11, and 0.98 ± 0.08 were obtained. 4-Nitrophenol, 4-nitrocatechol, 2-nitrobenzoic acid, and 2-nitrophenol showed mean retention coefficients of 1.01 ± 0.07, 1.01 ± 0.14, 0.99 ± 0.04, and 0.21 ± 0.12. Only the retention coefficient of 2-nitrophenol showed a dependence on temperature, growth regime, and pH. This is in accordance with previous studies which showed a dependence between the dimensionless effective Henry's law constant H^* and the retention coefficient for inorganic and small organic molecules. Our results reveal that this correlation can also be applied to more complex organic molecules, and that retention under these conditions is not a significant factor for molecules with H^* below 10^3, while retention close to 1 can be expected for compounds with H^* above 10^8.
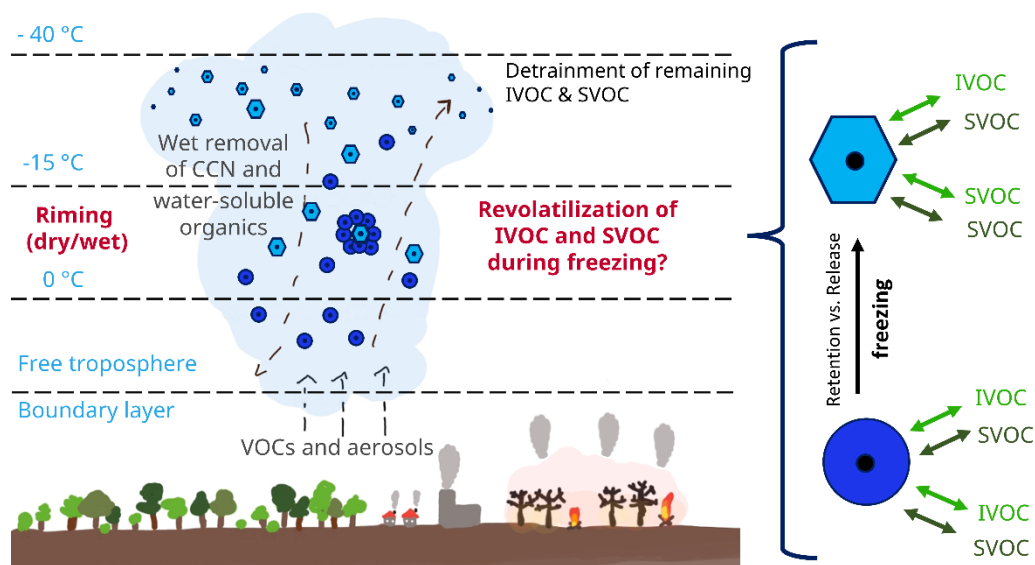
1 Introduction

The observation of a large number of small particles at high altitudes, which has already been made several times, is attributed to the formation of new particles (New Particle Formation, NPF) through the process of homogeneous nucleation and early

growth. The rate of NPF formation is strongly dependent on the concentration of low volatile vapors, the temperature and the number of particles that are present. Low-volatility vapors are for example sulfuric acid, which is formed from the reaction of sulfur dioxide and hydroxyl radicals or via oxidation of dimethyl sulfide, as well as highly oxidized organic compounds (Xiao et al., 2023; Williamson et al., 2019; Andreae et al., 2018; Kerminen et al., 2018; Twohy et al., 2002). A common explanation

35 for the presence of this high number of small particles at high altitudes is the uplift of condensable vapors with simultaneous removal of existing aerosol particles in deep convective clouds. This removal of larger particles reduces the sinks for small particles and condensable vapors, supporting NPF (Clarke et al., 1998). However, Williamson et al. (2019) showed that tropical convection does not lead to uniquely low particle numbers for larger particles. They then argue that there must be a stronger source of condensable vapors at high altitudes in the marine tropics than in other regions and that most of the models used

40 underestimated available organic matter at high altitudes and predict less NPF in these regions. It is therefore important to investigate the possible transport mechanism of organic precursor components that could lead to NPF at high altitudes (Bardakov et al., 2022).

Among other mechanisms, deep convection plays an important role in the transport of trace substances and aerosols into the upper troposphere. In this region, these substances have a longer atmospheric lifetime, thereby increasing the likelihood of

45 long-range transport. Additionally, they can contribute to NPF (Bardakov et al., 2022; Barth et al., 2007a; Barth et al., 2007b). The fraction that arrives in the upper troposphere is influenced by the liquid phase and mixed-phase scavenging of the substances. Aircraft measurements from the USA in thunderstorm inflow and outflow regions demonstrate that water-soluble trace gases, such as H_2O_2, are removed with efficiencies between 79% and 97%, which are also influenced by the process of retention (Bela et al., 2018; Barth et al., 2016).

50 Figure 1 shows vertical transport mechanisms of intermediate-volatile and semi-volatile organic compounds (IVOC and SVOC).

Organic compounds in the atmosphere can be categorized into different groups depending on their source, such as biogenic, anthropogenic, or compounds originating from the combustion of biomass (Gouw and Jimenez, 2009). Nitro-aromatic compounds can be formed directly from the combustion of coal or wood, but can also be formed as secondary products from the reaction of phenols or cresols with NOx (Wang et al., 2020; Harrison et al., 2005). Terrestrial vegetation emits large quantities of volatile organic compounds (VOCs) such as isoprene and various monoterpenes (MT), with the most important MT α-pinene contributing around one third of global MT emissions (Sindelarova et al., 2014). In the atmosphere, oxidation by OH radicals, ozone or NO_3 radicals results in various products spanning orders of magnitude in volatility. Products such as 2-methyl tetrols, pinanediol, terpenylic acid, pinonic acid, pinic acid, have been described as major oxidation products (Kołodziejczyk et al., 2020; Bianchi et al., 2019; Nozière et al., 2015; Müller et al., 2012; Kroll and Seinfeld, 2008; Claeys et al., 2004; Hoffmann et al., 1997). At standard conditions, the saturation vapor pressure of these oxidation products is too large for being relevant for new particle formation. Highly oxygenated organic molecules (HOMs) exhibit a sufficient low vapor pressure for NPF (Bianchi et al., 2019), however, their formation via autoxidation, a rapid OH-radical–induced oxidation process in the atmosphere, is suppressed at low temperatures (Stolzenburg et al., 2018). Hence, the higher-volatility major oxidation products of isoprene and monoterpenes might be relevant for NPF in the upper troposphere, where HOM formation is suppressed and the colder temperatures cause saturation of the major oxidation products, which are classified as SVOCs at standard conditions. Both classes of compounds focused on in this study, i.e. pinene oxidation products and nitro-aromatic compounds, are IVOCs (saturation mass concentration C^*: $300 < C^* < 3 \cdot 10^6 \, \mu g \, m^{-3}$) or SVOCs ($0.3 < C^* < 300 \, \mu g \, m^{-3}$) (Simon et al., 2020; Andreae et al., 2018).

Water-soluble IVOCs and SVOCs can be dissolved in water droplets (dark blue circles in Figure 1), which can be transported upwards via deep convection. In the mixed-phase zone of clouds, retention or release of IVOCs and SVOCs during riming can occur. Riming describes the collision and freezing of supercooled water droplets on the surface of hydrometeors such as a graupel or snowflakes (light blue hexagon in Figure 1) which leads to their growth. The organic compounds can be trapped in the ice phase and then washed out by precipitation, or they can return to the gas phase by volatilization during freezing. This revolatilization leads to a vertical redistribution in the atmosphere and could explain the occurrence of semi-volatile organic compounds at high altitudes in regions with deep convection. However, if the organic substances remain in the ice phase during freezing, they could also be transported further upwards and released into the gas phase by sublimation of the ice particles there (Pruppacher and Klett, 2010; Snider and Huang, 1998).

The proportion of the compound that remains in the ice can be described by the retention coefficient R, which indicates the relative fraction of the trapped compound with a value between 0 and 1 (Bela et al., 2018; Stuart and Jacobson, 2003; Snider et al., 1992; Iribarne and Pyshnov, 1990). The retention of a compound is influenced by its chemical properties, such as the dimensionless effective Henry's law solubility constant H^*, as well as physical parameters such as temperature, droplet size,

liquid water content in the cloud, ventilation, and potentially the pH of the droplet, which also influences H^*. Compounds with a small H^* are more likely to return to the gas phase during riming, which results in a lower retention coefficient. In addition, external conditions have a greater influence on retention for these kind of compounds, which is in contrast to compounds with high H^* (Cuchiara et al., 2023; Jost et al., 2017; Stuart and Jacobson, 2004, 2003).

Previous measurements of inorganic and small organic species in the wind tunnel in Mainz confirm the correlation between H^* and R as well as the stronger dependence of retention on external factors such as temperature for lower H^*. Hydrochloric acid, nitric acid, malonic acid, and oxalic acid are characterized by a high H^* value and remain completely in the ice phase during freezing. Compounds with more moderate H^* values such as ammonia, hydrogen peroxide, formic acid, and acetic acid have retention factors of 0.92 ± 0.21, 0.64 ± 0.11, 0.68 ± 0.09, and 0.72 ± 0.16. Retention of the organic compounds show a dependence on temperature and ventilation. Additionally, sulfur dioxide shows both the lowest H^* value and retention coefficient (0.46 ± 0.16) of the compounds discussed as well as with a dependence on external conditions (Jost et al., 2017; v. Blohn et al., 2013; 2011).
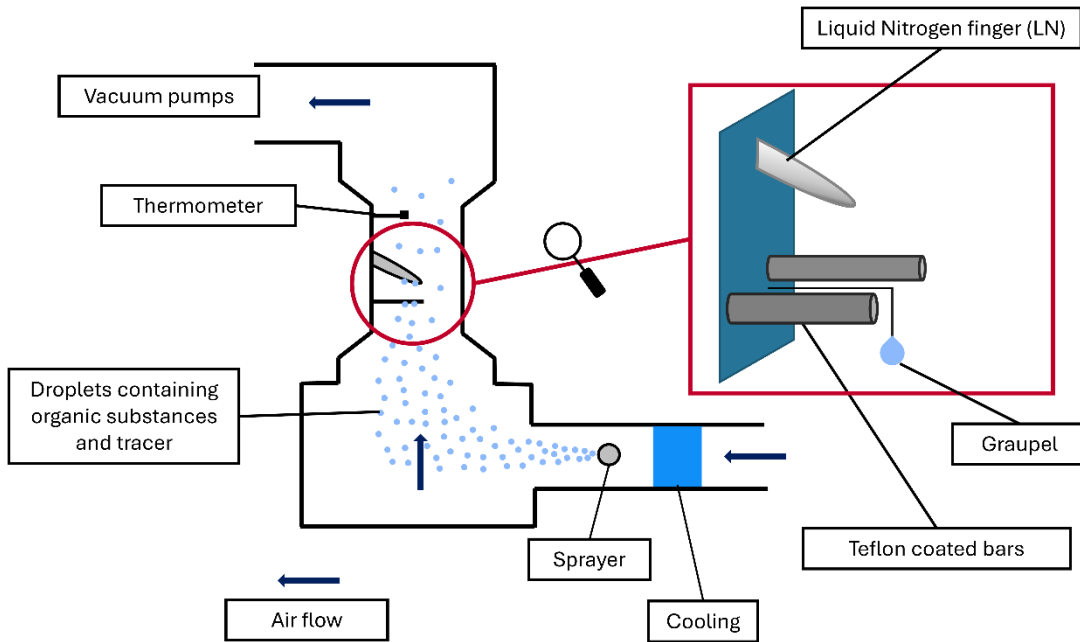
Up to now, only inorganic, and small organic molecules have been investigated with regard to their retention during the freezing process. Measurements of rain, hail and cloud water have already shown that they contain α-pinene oxidation products and nitrophenols (Spolnik et al., 2020; Desyaterik et al., 2013; Ganranoo et al., 2010). It is therefore likely that these compounds are also present in the supercooled droplets within mixed phase zones of clouds. In contrast to the smaller organic molecules and inorganic compounds, the retention coefficients for α-pinene oxidation products and nitrophenols are unknown. In this study, therefore, the retention coefficients of three α-pinene oxidation products (pinonic acid, pinic acid, and pinanediol) and four nitro-aromatic compounds (2-nitrobenzoic acid, 4-nitrocatechol ,4-nitrophenol, and 2-nitrophenol) are investigated in a series of wind tunnel experiments under simulated atmospheric conditions.

2 Experimental procedures

2.1 Mainz vertical wind tunnel

The experiments were carried out in the vertical wind tunnel of the Johannes Gutenberg University of Mainz, shown schematically in Figure 2. Here, hydrometeors ranging from a few tens of micrometers to centimeters can float freely in a vertical air stream at their terminal fall velocity. The prevailing conditions such as ventilation, mass, and heat transfer are very similar to those in the atmosphere (Pruppacher and Klett, 2010). A vacuum pump continuously sucked dried ambient air through the system to produce an air flow in the wind tunnel. For riming experiments the tunnel was cooled down to $-18\ °C$ and water droplets were produced using up to four spray nozzles. These droplets were transported via the airflow to the experimental region (red circle, zoomed in: red rectangle in Figure 2). In the experimental region the supercooled droplets collided with three different surfaces—a simulated graupel, a liquid nitrogen finger, and Teflon-coated bars— and froze on

the substrate. A detailed description of the experiments is provided in Sect. 2.3 Retention measurements. Further details on the wind tunnel can be found in two reviews by Diehl et al. (2011) and Szakáll et al. (2010).

Figure 2: Schematic of the wind tunnel. Cooled air transported the generated water droplets containing the compounds into the experimental region (red circle). Red rectangle: The enlarged experimental area shows the three surfaces on which the riming took place: Graupel, liquid nitrogen finger and Teflon-coated bars.

2.2 Growth regimes

For riming, a distinction is made between dry and wet growth conditions, which are determined by the combination of
125 temperature, liquid water content and ventilation. During freezing latent heat is released, which warms the surface of the rime collectors. Under dry growth conditions the surface temperature of the rime collector remains well below 0 °C and all the accreted cloud water freezes within some milliseconds on the rime collector, preserving a close to spherical shape. The surface temperature increases with increasing liquid water content, droplet size, and collision frequency of the droplets with the hydrometeor. If the temperature rises to a maximum value of 0 °C wet growth conditions are reached. At this point, not all the
130 water that has collided with the rime collector freezes immediately. During wet growth, the freezing rate of an element of liquid input is rather low in comparison to dry growth conditions, resulting in a dense ice structure (Pruppacher and Klett, 2010; Macklin, 1961; List, 1960).

The earlier wind tunnel measurements on retention coefficients (Jost et al., 2017; v. Blohn et al., 2013; 2011), focused solely on retention during dry growth conditions. Thus, there remained the question to which extent wet growth conditions affect
135 retention. For example, Michael and Stuart (2009) found in their theoretical study that during wet growth conditions H^* is an important but not a dominant factor. They observed that retention increased with increasing H^* (from 300 to $3 \cdot 10^6$) and then

5

leveled off with further increasing H^*, resulting in low retention values for compounds with high H^* such as HCl. Here other factors like the ice-liquid interface supercooling and the liquid water content are major determinators for the extent of retention. In the present study, the measurements were carried out at dry and wet growth conditions. However, unlike the study of
140 Michael and Stuart (2009), it was not observed that the droplets shed off during these experiments. Calculations of the surface temperature during the growth of graupel reveals that under our wet growth conditions the surface temperature varied between −0.8 and −2.2 °C for −3 and −5 °C ambient temperature respectively and had a measured LWC of 2.2 g m^{-3} (Theis et al., 2022; v. Blohn et al., 2009; Pflaum and Pruppacher, 1979). For temperatures higher than −3 °C, no freezing was observed on the Teflon-coated bars and little freezing could be observed on the graupel. During wet growth experiments small cloud
145 droplets coalesced and formed larger mm-sized drops before freezing. A photo of an example ice sample is provided in the Supplement (Figure S1). This coalescence of droplets during our experiments are representative of the wet growth of graupel rather than the wet growth of hail—where the accreted liquid water is shed off from the surface due to the faster fall speeds.

2.3 Retention measurements

Dilute aqueous solutions with different compositions were used for the experiments. Single component measurements were
150 carried out for the α-pinene oxidation products and 2-nitrophenol. The aqueous solution to be analyzed contained one of the compounds of interest (pinonic acid, pinic acid, pinanediol, or 2-nitrophenol) and sodium bromide (NaBr; Sigma-Aldrich/ ≥99 %). For the other nitro-aromatic compounds (2-nitrobenzoic acid, 4-nitrocatechol, and 4-nitrophenol), a mixture of all organics and NaBr was used, an experimental setup that comes closer to the complex conditions in the atmosphere. All samples contained NaBr as an internal standard (IS) to account for dilution and evaporation effects. The retention of NaBr is assumed
155 to be 1, i.e. NaBr remains completely in the droplets during freezing. HCl (30 %) was added if the measurements were carried out at a pH value of 4. The concentrations of the chemicals used is shown in Table 1.

Table 1: Concentrations of the investigated solutions.

Compound	Concentration (µmol L^{-1})	Label /purity	IS concentration NaBr (µmol L^{-1})
cis-pinonic acid	10	Sigma Aldrich/98 %	10
cis-pinic acid	10	Synthesized/N/A	10
(1R,2R,3S,5R)-(−)-pinanediol	15	Merck/99 %	10
2-nitrophenol	30	Thermo Scientific/99 %	10
2-nitrobenzoic acid	10	Thermo Scientific/95 %	10
4-nitrocatechol	10	Thermo Scientific/≥98 %	10
4-nitrophenol	10	Alfa Aesar/99 %	10

To generate the supercooled droplets, the solution containing the analyte and the IS was nebulized with a gas stream of nitrogen (>99.8 %) and either two or four spray nozzles depending on the experiment. Two spray nozzles and a nitrogen flow of 20 L min^{-1} were used for dry growth and four spray nozzles and a flow of 24 L min^{-1} for wet growth conditions. The number of spray nozzles influences the liquid water content (LWC) and thus the growth regime.

For dry growth conditions a lower LWC is required, therefore only two spray nozzles were used. The resulting droplet size distribution in the wind tunnel was measured using a custom in-line digital holographic instrument, similar to the "holographic imaging and velocimetry instrument for small cloud ice" (HIVIS) described by Weitzel et al. (2020). The measurements were not taken simultaneously to each retention experiment but measured independently under the same conditions during the retention experiments. After the cloud of droplets was produced, a camera (Basler acA2040) captured the holograms containing the images of the droplets at 90 fps. Typical measurement time was 1 minute. Approximately 5400 holograms were reconstructed and analyzed for each measurement with two and four nozzles. Using a telecentric lens with a 0.5 magnification, the pixel size of the holograms was 2.72 µm x 2.72 µm which yielded a sample area and volume of 5.57 x 5.57 mm^2 and 2.48 cm^3 respectively. For the reconstruction of the holograms, a depth of 8 cm was chosen as this represents the central part of the measurement section where the collectors were exposed to the cloud of supercooled droplets during experiments. The holograms were reconstructed at each $\Delta z = 100$ µm distance along the optical axis using the method of Fugal et al.(2004). This produced an in-focus image of the droplets independent of their location within the sample volume. The particle sizes were obtained from a particle detection algorithm of Fugal et al. (2009), which determined the normalized number and volume distributions. Figure 3 (a) shows the number distribution of the supercooled droplets in the measurement section of the tunnel when two spray nozzles were used. Figure 3 (b) shows the volume distribution of the droplets, which represents the normalized cloud liquid water content (LWC) per size interval. We observed no difference in the distribution when using four nozzles (see SI Figure S2). The LWC was measured using a dew-point meter (MBW Calibration Ltd., Wettingen, Switzerland, DP3-D/SH) in conjunction with a 5 m long heated pipe. Wind tunnel air was sampled isokinetically through the heated pipe to evaporate the droplets. The absolute humidity was then obtained from the dew point measurement. In a second step, a droplet separator was installed at the inlet to the heated tube to measure the dew point of the wind tunnel air without droplets. The difference between the two absolute humidities gives an LWC of 0.9 ± 0.2 g m^{-3} for dry growth and 2.2 ± 0.2 g m^{-3} for wet growth conditions.
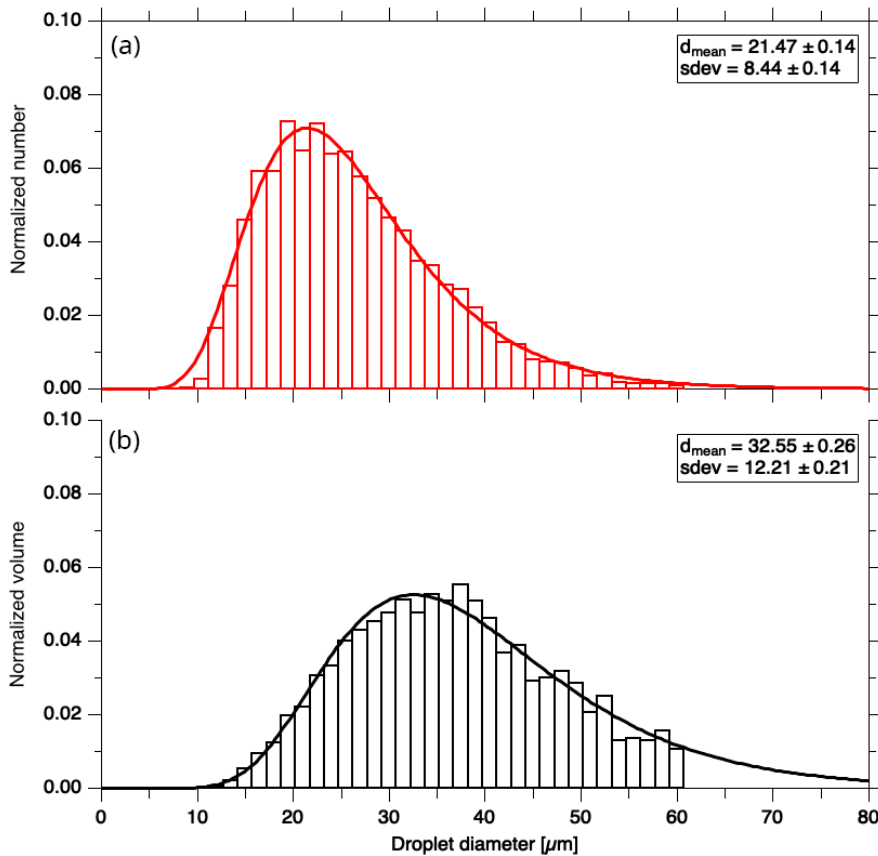
Figure 3: Normalized droplet number (a) and volume distribution (b) of the supercooled droplets generated using two spraying nozzles. The lines represent log-normal fit functions.

During retention measurements, the droplets were transported downstream from the sprayer into the experimental section. The distance between the sprayer and the experimental region is approx. 3 m (Jost, 2012). In the experimental section, the supercooled droplets collided with three different surfaces, which were used as rime ice collectors and froze on them. The first surface was a Teflon-coated bar (FEP; outer diameter 6 mm) and the second was an ice sphere (graupel) with a diameter of 7 mm, which comes closer to real atmospheric sizes for graupel. According to the American Meteorological Society glossary of meteorology, graupel are defined as rimed particles with diameters less than 5 mm; larger ones are called hailstones. However, we refer to the investigated particle as graupel according to the flow conditions present rather that of particle size. The larger diameter was necessary to obtain a sufficient sample volume for analysis. The last surface was a cold tube made of Teflon (PFA) that was constantly filled with liquid nitrogen (LN finger tube). This sample determined the liquid phase concentration of the droplets immediately before riming occurs. At the surface of the LN finger tube, freezing is so fast that the retention can be assumed to be 1 and the concentration of the droplets can be determined before riming.

To produce the simulated graupel, a silicon mold was filled with ultra-pure water and frozen. The graupel were "captively floated" to avoid the loss of graupel and any contamination on contact with the wind tunnel walls. For this purpose, they were

attached to a nylon fiber with a diameter of 80 µm. Under these conditions, the rime collectors were exposed to the airflow containing the supercooled droplets at 3 m/s, which corresponds to a typical fall velocity of a graupel. (Wang and Kubicek, 2013; Pruppacher and Klett, 2010). The ice samples were collected after each experimental run and stored at -25 °C until they were melted for the chemical analysis.

2.4 UHPLC-HRMS analysis

For analysis, the ice samples were melted and filtered through polyamide (PA) membranes (pore size: 0.20 µm; Altmann Analytik) to remove potential particles, but without affecting the concentration of the analytes. Analysis was performed in triplicate using a Dionex UltiMate 3000 ultra-high-performance liquid chromatography (UHPLC) system coupled to a heated electrospray ionization source (HESI) or atmospheric pressure chemical ionization (APCI), and a high-resolution Q-Exactive Orbitrap mass spectrometer (HRMS) (all Thermo Fisher Scientific). A Hypersil Gold, C18, 50 x 2.0 mm column with 1.9 µm particle size (Thermo Fisher Scientific) was used for the chromatography. Eluent A consisted of 98 % LC/MS grade water (Thermo Fisher Scientific) with 0.04 % formic acid and acetonitrile (VWR Chemicals), eluent B consisted of 98 % acetonitrile and water, and the injection volume was 5 µL. Different H_2O/ACN gradients were used for the different compounds. For pinonic acid, pinic acid, pinanediol, 2-nitrobenzoic acid, 4-nitrocatechol, and 4-nitrophenol, a flow rate of 0.5 mL min^{-1} and a gradient as described following were used: Starting with 2 % B isocratically for 1 min, increasing to 20 % B in 2.5 min, then further increasing to 90 % in 1.5 min, after which B was held at 90 % for 4 min, decreased to 2 % in 0.5 min, and held again for 1.5 min. For pinanediol, a post-column flow of 50 mmol L^{-1} NH$_4$OH in MeOH was added after 1 min at a flow rate of 0.1 mL min^{-1} to enhance ionization. The HESI source was used in negative mode, resulting in the formation of deprotonated molecular ions. Sheath gas and auxiliary gas flow was 40 and 20 a. u.(arbitrary unit) respectively. The temperature of the auxiliary gas heater was 150 °C and the capillary temperature was 350 °C. The sprayer voltage was set to -4.00 kV.

A different gradient with a flow rate of 0.3 mL min^{-1} was used for 2-Nitrophenol. Starting with 2 % B isocratically for 1 min, increasing to 20 % B in 2.5 min, then further increasing to 90 % in 1.5 min, after which B was again held at 90 % for 0.3 min, decreased to 2 % in 0.2 min and held again for 0.5 min. To further enhance ionization, a post-column flow of 50 mmol L^{-1} NH$_4$OH in MeOH was added after 1 min at a flow rate of 0.1 mL min^{-1}. The APCI source was used in negative mode, resulting in the formation of deprotonated molecular ions. Sheath gas and auxiliary gas flow was 23 and 5 a. u., respectively. The vaporizer temperature was 375 °C and the capillary temperature was 350 °C.

2.5 Calculation of the retention coefficient

Eq. (1) was used for compounds with a retention coefficient R close to 1:

$$R = \frac{c_{\text{compound}}^{\text{sample}} / c_{\text{compound}}^{\text{LN}}}{c_{\text{IS}}^{\text{sample}} / c_{\text{IS}}^{\text{LN}}} \tag{1}$$

The numerator describes the ratio between the concentration of the compound of interest in the ice sample ($c_{\text{compound}}^{\text{sample}}$) (Teflon coated bars or graupel) and in the LN finger sample ($c_{\text{compound}}^{\text{LN}}$). The denominator describes the same ratio but for the IS ($c_{\text{IS}}^{\text{sample}}$ / $c_{\text{IS}}^{\text{LN}}$). Thus, it is not necessary to consider a dilution, evaporation, and desorption correction as these effects change

235 both the compound and IS concentration in the nitrogen finger sample accordingly. Therefore, a change in this ratio is solely an effect of the retention of the compound during the riming process.

The calculation is different for compounds with a lower effective Henry's law constant (below 10^4), which leads to higher desorption. These compounds are transferred to the gas phase in larger amounts before and during the freezing process, resulting in a higher gas phase concentration in the tunnel. Therefore, it cannot be ruled out that the measured concentrations

240 of the LN finger tube samples could be influenced by additional adsorption out of gas phase components. This would no longer provide a suitable correction for determining the retention coefficient.

As the LN finger sample is not available, the sprayer sample (the solution from which the droplets are produced) is used instead. As the distance between the two sampling points (sprayer and graupel/bar) is large, it is necessary to determine the amount of compound that is transferred to the gas phase before freezing. The desorption correction coefficient D (see

245 Supplement (Eq S3)) will be utilized. A detailed description of the desorption correction coefficient can be found in the Supplement.

To calculate the retention coefficient R for compounds with a lower retention coefficient, Eq. (1) was extended to include the desorption correction coefficient using the sprayer solution sample instead of the LN finger (see Eq. (2)):

$$R = \frac{c_{\text{compound}}^{\text{sample}} / c_{\text{compound}}^{\text{sprayer}}}{c_{\text{IS}}^{\text{sample}} / c_{\text{IS}}^{\text{sprayer}} \cdot D} \qquad (2)$$

250 Equation 1 and 2 yield identical results for compounds with a desorption correction coefficient of approximately 1. This is illustrated using pinic acid as a representative example in the Supplement (Figure S3).

3 Results and discussion

3.1 Retention measurements

The results of the retention measurements for the α-pinene oxidation products are shown in Figure 4; those for 4-nitrocatechol,

255 nitrobenzoic acid, and 4-nitrophenol are shown in Figure 5; and the desorption corrected R for 2-nitrophenol in Figure 6.
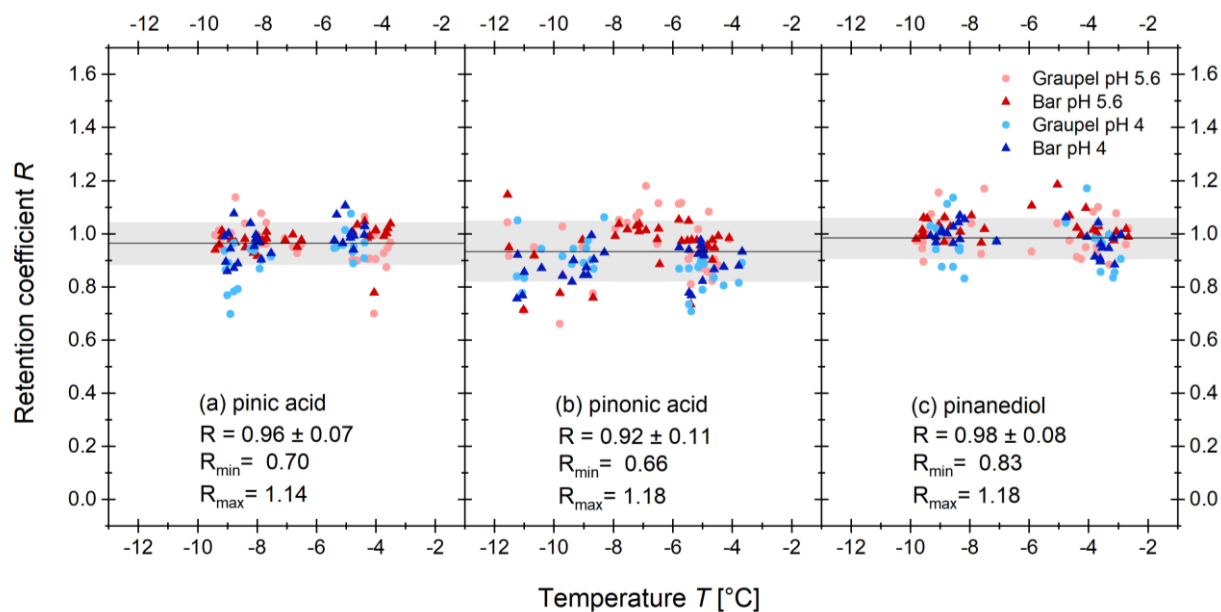
Figure 4: Experimentally determined retention coefficients of (a) pinic acid, (b) pinonic acid, and (c) pinanediol as a function of the temperature during the experiment for different rime collectors. The circles represent the graupel samples and the triangles those of the Teflon-coated bars. For the blue symbols, the pH was adjusted to 4 by adding HCl (30 %), the red symbols are without adding HCl. The solid black line represents the mean of all measurements, and the grey area represents one standard deviation.

3.1.1 Pinic acid and pinonic acid

Figure 4 shows the results for (a) pinic and (b) pinonic acids. Pinic acid and pinonic acid both show neither a pH or temperature dependence nor influence from the rime regime. This agrees with the earlier findings for compounds with high H^*. The retention coefficients for pinic acid vary between 0.65 and 1.14 with a mean value of 0.96 ± 0.08. For pinonic acid, a mean retention coefficient of 0.92 ± 0.10 was determined. The variation in the measured values of R is greater than that for pinic acid and lies between 0.66 and 1.18. This is probably due to the lower H^*, which makes pinonic acid more sensitive to slight changes in the experimental conditions. The scatter of the values is comparable to that observed in other studies on retention. Theoretical and experimental studies have demonstrated that the retention of compounds with a low H^* is dependent on the freezing conditions (Jost et al., 2017; v. Blohn et al., 2013; 2011; Stuart and Jacobson, 2004, 2003). The results shown here indicate that slight differences in freezing conditions across the experiments may exert an influence on the retention of compounds, despite their high H^* values.

3.1.2 Pinanediol

The results for pinanediol are depicted in Figure 4 (c). No effect on the investigated parameters could be found for this diol. The mean retention coefficient was 0.98 ± 0.08 with a minimum value of 0.83 and a maximum value of 1.18, which is an exception to previous findings (Jost et al., 2017). In comparison to pinic and pinonic acid, pinanediol showed a lower H^* (see

11

Table 3). A lower retention coefficient is expected for compounds in this range as well as a dependence on temperature. However, no temperature, pH, or growth regime dependence was seen. This deviation from the expected behavior could be because the Henry's law constant for pinanediol is estimated using the bond method implemented in the HENRYWIN[TM] software as part of EPI Suite[TM]. The bond method breaks down the molecule into a sum of the individual bonds that make up

280 the compound. The exact structure and spatial orientation of the molecule is not considered. Due to the large deviations of the polyols in the original method by Hine and Mookerjee (1975), further correction factors were included in the method. However, the predictions are less accurate for molecules with a more complex structure (Meylan and Howard, 1991; Hine and Mookerjee, 1975). Pinanediol is a cyclic diol. Due to its capped ring form, it is sterically hindered and thus the potential interactions between the OH groups are not considered by the model. Since there is no experimental data for the Henry's law constant,

285 there is no current alternative to the estimation.

3.1.3 4-Nitrocatechol and 4-nitrophenol

The results for 4-nitrocatechol and 4-nitrophenol are shown in Figure 5 (a) and 5 (b). Overall, no pH or temperature dependence is recognizable. Furthermore, no difference between wet and dry growth conditions can be observed. This agrees with the current literature. As Stuart and Jacobson (2004, 2003) have shown, a temperature or pH dependence is not expected for

290 compounds with high effective Henry's law constants, such as 4-nitrocatechol or 4-nitrophenol. A mean retention coefficient of 1.01 ± 0.14 and 1.01 ± 0.07 was determined for 4-nitrocatechol and 4-nitrophenol respectively. For 4-nitrocatechol, the derived retention coefficients showed a large scatter that has no current explanation. A minimum value of 0.63 and a maximum value of 1.41 was obtained. 4-nitrophenol showed a smaller scatter with values between 0.79 and 1.28.
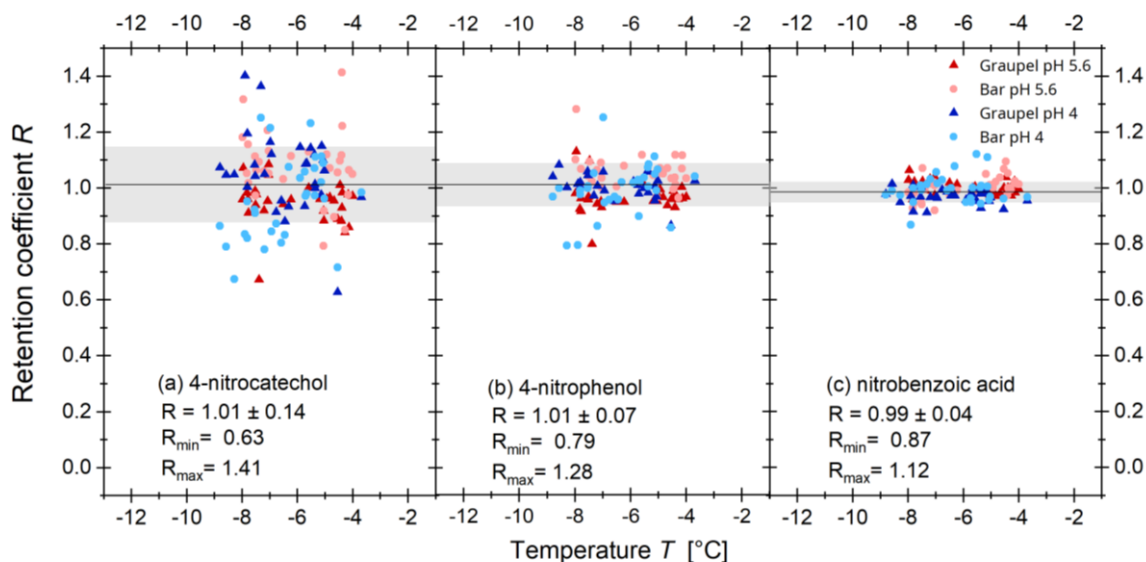

295 **Figure 5: Experimentally determined retention coefficients of (a) 4-nitrocatechol, (b) 4-nitrophenol, and (c) nitrobenzoic acid as a function of the temperature during the experiment for different riming collectors. The circles represent the graupel samples and the**
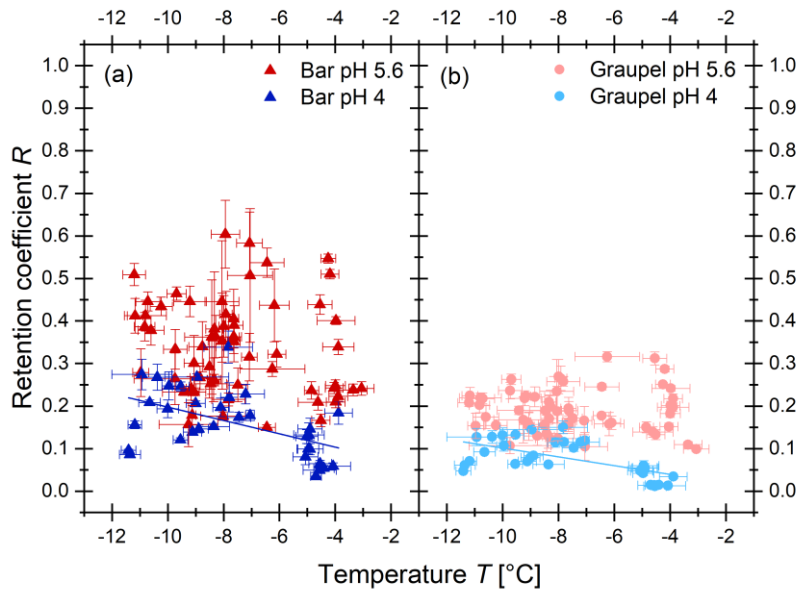
12

triangles those of the bars. For the blue symbols, the pH was adjusted to 4 by adding HCl (30 %), the red symbols are without adding HCl. The black line represents the mean of all measurements, and the grey area represents one standard deviation.

3.1.4 2-Nitrobenzoic acid

300   For 2-nitrobenzoic acid in Figure 5 (c), no dependence on the investigated parameters was found. The average retention coefficient is 0.99 ± 0.04, with the lowest scatter among the measured compounds. The smallest value measured was 0.87 and the largest 1.12. This is probably because 2-nitrobenzoic acid has the lowest pKa value of all the compounds studied. In the pH range investigated, most of the 2-nitrobenzoic acid molecules are deprotonated, unlike the other components studied. This makes a transition into the gas phase less likely and therefore small differences in the measurement conditions have less

305   influence on the results.

3.1.5 2-Nitrophenol

2-Nitrophenol (Figure 6) showed significantly lower retention coefficients than the other compounds presented above. The retention coefficients shown here are desorption corrected according to Eq. 2. At pH 4the different rime collectors (Teflon-coated bar, graupel) showed a statistically significant (significance level $\alpha = 0.05$) negative temperature dependence (lines

310   and equations in Figure 6; Table 2).. The bar samples show a slightly stronger temperature dependence than the graupel samples. This is probably due to the metal rod inside the Teflon-coated bar and the resulting faster heat transfer. It is also noticeable in these measurements that the graupel samples (light red and light blue circles in Figure 6 (b)) have an overall lower retention coefficient than the bar samples (red and blue triangles in Figure 6 (a)). This might also be explained by the metal rod inside the Teflon-coated bar. The faster heat transfer leads to a shorter freezing time and thus to a higher retention

315   coefficient. At a pH value of 5.6, no statistically significant negative temperature trend could be determined. This could be attributed to the greater scattering of the values, which is presumably caused by fluctuations in the conditions in the wind tunnel and slight variations in the pH value of the solution utilized. The fluctuation of the values could conceal an existing temperature trend.

Figure 6: Experimentally determined desorption corrected retention coefficients of 2-nitrophenol as function of the temperature during the experiment for different rime collectors. The triangles represent the Teflon coated bar samples (a) and the circles those of the graupel (b). For the blue symbols, the pH was adjusted to 4 by adding HCl (30 %), the red symbols are without adding HCl. The line represents a linear fit.

The data points (Figure 6) below −6 °C were obtained from dry growth conditions, while the ones higher than that represent wet growth conditions. A closer inspection of the data reveals that the temperature dependency might also be a result of the riming regimes. When separating the data between the two regimes the temperature dependency vanishes. Therefore, the difference in retention values between wet and dry growth conditions might be due to the longer freezing times of the accreted and coalesced droplets. The droplets accreted during wet growth regime remained liquid for some time and formed a larger mm-size drop before they froze. This means dissolved 2-nitrophenol could further desorb from the drops before ice shell formation occurred, which reduces further expulsion from the freezing droplet. This resulted in slightly lower retention values for the rime collectors grown during wet growth. Considering the absolute retention values for wet growth, it becomes apparent that 2-nitrophenol will not retain in atmospherically significant amounts during wet growth conditions. However, as the values between dry and wet growth overlap within the experimental uncertainty, a temperature dependency is provided here, which is applicable within the investigated temperature and growth conditions range simulated in the present study. As the temperature dependence in the analyzed range has only a minor influence on the retention compared to the data scattering, the mean values were determined for all sets of measurements. The mean retention coefficients for the various riming conditions are shown in Table 2. The overall mean retention coefficient was determined to be 0.21 ± 0.12. The measured values of R were between a minimum of 0.01 and a maximum of 0.60.

14

In addition to the dependence on temperature, growth regime, and the riming collectors already discussed, the pH dependence
340   was also analyzed as retention is also strongly dependent on the dissociation of the molecules. As the retention for the rime collectors is different, the comparisons are only carried out within the same collectors. The mean retention coefficients for the graupel samples at pH 5.6 and pH 4 were 0.19 ± 0.05 and 0.08 ± 0.04 respectively. At pH 5.6 it is more likely that 2-nitrophenol is dissociated in comparison to pH 4. A dissociated molecule needs to be neutralized by a proton before leaving the droplet during riming. At pH 5.6, more molecules are available that do not evaporate without recombination which might
345   explain the higher retention coefficient.

Table 2: Measured retention coefficient of 2-nitrophenol and their temperature dependencies.

Conditions	Mean retention coefficient R	Temperature dependency of R
Bar pH 5.6	0.34 ± 0.11	-
Graupel pH 5.6	0.19 ± 0.05	-
Bar pH 4	0.16 ± 0.07	$R_{B_4} = (-0.016 \pm 0.005)\,T + (0.041 \pm 0.037)$
Graupel pH 4	0.08 ± 0.04	$R_{G_4} = (-0.010 \pm 0.002)\,T + (-0.002 \pm 0.019)$

3.2 Relationship between Henry's law constant and retention

350   Jost et al. (2017) have shown a correlation between the retention coefficient R and the dimensionless effective Henry's law constant H^* ($H^* = K_H \cdot \bar{R}T$, with K_H: effective Henry's law constant; $\bar{R}$: gas constant; T: temperature) for inorganic and small organic molecules, which can be described by Eq (3).

$$R(H^*) = \left(1 + (a\,/\,H^*)^b\right)^{-1}, \tag{3}$$

where R is the retention coefficient, H^* is the dimensionless effective Henry's law constant and a and b constants that are
355   determined by a fit. To test whether this relationship is also applicable to the larger organic molecules investigated here, the mean values of retention coefficients of the compounds were plotted against their dimensionless effective Henry's law constant (Figure 7). H^* was determined for the investigated pH values and at 298 K. Since most of the compounds analyzed in this study did not show any pH dependence within the pH range of 4 and 5.6, a pH value of 4 was used for the calculation of H^* for these compounds. This is a typical value found in cloud water samples (Pye et al., 2020; Löflund et al., 2002). For 2-
360   nitrophenol, the mean retention coefficient for each of the pH values (pH 4 and 5.6) were calculated and plotted (Figure 7). The fact that a pH dependence was only found for 2-nitrophenol is consistent with the literature. A pH dependence is only to be expected for compounds with low H^*. Additionally, a dependence is expected primarily in a pH range near the pKa value, as the impact on the ratio between dissociated and non-dissociated molecules is most pronounced in this range (Reijenga et al., 2013; Stuart and Jacobson, 2003). The pKa values of pinic acid and pinonic acid are the most similar to the investigated

15

365 pH values. However, the $H*$ values seem to be too high to detect an influence of pH on the measurements. The calculated values of $H*$ are listed in Table 3. Since there are no measured Henry's law constants nor reaction enthalpies for some of the more complex organic compounds, these were predicted using the bond method of the HENRYWIN[TM] software which provides the values for 298 K.

370 **Table 3: Retention coefficient of the measured compounds, their pK$_a$ values, Henry's law constants, and dimensionless effective Henry's law constants at 298 K and pH 4 for all compounds except 2-nitropheand (pH 4 and 5.6).**

Compound	Mean retention coefficient R	Acid dissociation constant pK$_a$	Henry's law constant[1] / M/atm	dimensionless effective Henry's law constant
4-nitrocatechol	1.01 ± 0.14	7.23[2]	$4.35 \cdot 10^9$	$1.06 \cdot 10^{11}$
2-nitrobenzoic acid	0.99 ± 0.04	2.17[3]	$2.08 \cdot 10^6$	$3.49 \cdot 10^9$
cis-pinic acid	0.96 ± 0.07	4.64[2]	$1.02 \cdot 10^8$	$3.06 \cdot 10^9$
cis-pinonic acid	0.92 ± 0.11	5.19[4]	$1.12 \cdot 10^6$	$2.93 \cdot 10^7$
4-nitrophenol	1.01 ± 0.07	7.15[3]	$4.52 \cdot 10^5$	$1.11 \cdot 10^7$
(−)-pinanediol	0.98 ± 0.08	14.68[2]	$4.08 \cdot 10^3$	$9.97 \cdot 10^4$
2-nitrophenol (pH 5.6)	0.27 ± 0.11	7.23[3]	$1.43 \cdot 10^2$	$3.50 \cdot 10^3$
2-nitrophenol (pH 4)	0.12 ± 0.07	7.23[3]	$1.43 \cdot 10^2$	$3.58 \cdot 10^3$

[1] Calculated using US EPA. [2012]. Estimation Programs Interface Suite™ for Microsoft® Windows, v 4.11. United States Environmental Protection Agency, Washington, DC, US; [2] Calculated using Advanced Chemistry Development (ACD/Labs) Software V11.02 (© 1994-2024 ACD/Labs); [3] (Haynes, 2014); [4] (Kołodziejczyk et al., 2019).

375

The compounds measured in this study are the colored, filled symbols in Figure 7; the ones measured by Jost et al.(2017), v. Blohn et al. (2013; 2011) and in earlier investigations in the wind tunnel are the grey, half-filled symbols. The grey dashed line represents the fit for the grey, half-filled symbols, i.e. previous measurements. Since the retention of formaldehyde, as shown in Jost et al. (2017), depends not only on $H*$ but also on the hydration to the diol, the value is not taken into account 380 when determining the fit. The resulting parameters are $a_{grey} = (2.41 \pm 1.06) \cdot 10^4$ and $b_{grey} = 0.27 \pm 0.04$. The red solid line is the new fit function in which all compounds are considered. Here again formaldehyde was not included into the fit. Pinanediol was also excluded from the fit as it appears to be an outlier (see Sect. 3.1.2). The values $a_{red} = (3.34 \pm 1.61) \cdot 10^4$ and $b_{red} = 0.36 \pm 0.06$ result for the fit function.
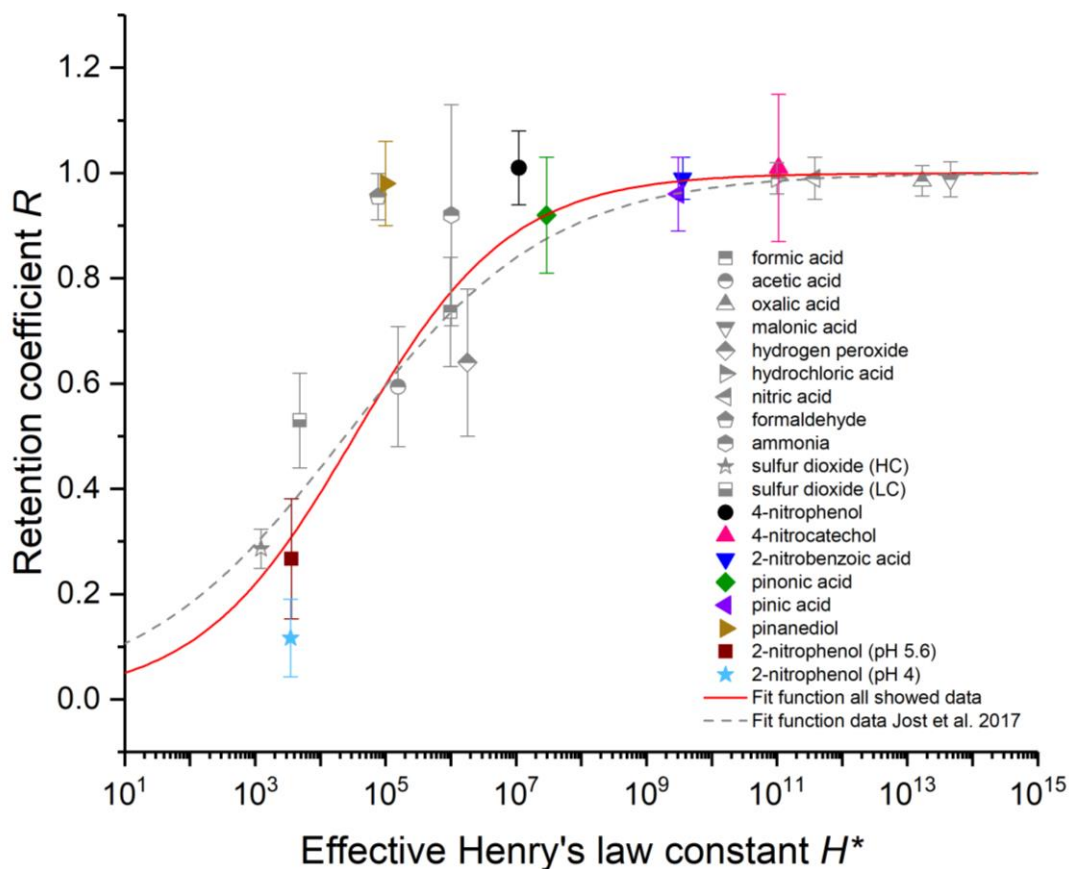
Figure 7: Measured retention coefficient as a function of H^*. Colorful filled symbols: compounds investigated in the present study. Grey symbols: wind tunnel data from earlier studies (Jost et al., 2017; v. Blohn et al., 2013; 2011) Red solid line: new fit to wind tunnel data. Grey dashed line: fit of the grey data points only.

As Figure 7 shows, the retention coefficients of larger organic molecules do also scale with H^* which agrees with the previous measurements. Only pinanediol and formaldehyde do not fit at first glance. A comparison of the new fit function (red solid line) with the values already known from the literature (grey dashed line) shows that the inflection in the fit function is steeper than previously assumed. Our results show that the retention of compounds with an H^* below 10^3 is close to 0, i.e. most of the compound dissolved in water is released into the gas phase during riming. This is also evident from the equilibrium distribution of species between the liquid and gas phase in a confined system, which is a function of the LWC (see Supplement Figure S9). For species with $H^* < 10^4$ just a maximum of 10 % is present in the liquid droplets even for LWCs of up to 10 g m^{-3}, which are only reached within severe storms (Lohmann et al., 2020). For $H^* > 10^3$ the compounds are present in significant amounts. For compounds with an H^* value above 10^8, a retention of 1 is expected with most of the compound remaining in the ice phase during freezing. This finding is in accordance with the literature. Stuart and Jacobson (2004) suggest a threshold value between 10^6 and 10^{10} M/atm for dry growth riming, which is in the same order of magnitude as the values presented here. For the

17

compounds in-between 10^3 and 10^8, the retention coefficient is highly dependent on H^*. However, the retention estimation is still afflicted with some degree of uncertainty especially in this H^* range. A close inspection of the data shows that it is not obvious that pinanediol and formaldehyde are outliers. It might also be that the transition from low to high retention values occurs in a smaller range of H^* and retention is 1 already for $H^* > 10^5$. We cannot ultimately clarify the steepness of the curve and the limiting regimes might be closer than assumed here. Jost et al. (2017) argued that formaldehyde cannot be explained solely by H^* and aqueous phase kinetics must be considered. However, such explanations are lacking for pinanediol. This might indicate that the transition from low to high retention values occurs at lower H^*. Support for that is given from the fit when taking all measurements into account, i.e. also formaldehyde and pinanediol (see Supplement Figure S10). To finally answer the question about the transition behavior of the function, further retention measurements in the range $10^4 < H^* < 10^6$ are needed. However, to our current knowledge, and particularly because of the lack of reliable measurements of H^* for pinanediol, we believe that the parameterization given above (Eq. (3), with $a_{\text{red}} = (3.34 \pm 1.61) \cdot 10^4$ and $b_{\text{red}} = 0.36 \pm 0.06$ is most trustworthy to calculate retention in the transition regime.

4 Conclusions

Wind tunnel experiments were carried out in the vertical wind tunnel of the Johannes Gutenberg-University Mainz to determine the retention coefficients R of three α-pinene oxidation products and four nitro-aromatic compounds. The experiments were performed in the temperature range from -12 to -3 °C with a liquid water content of $0.9 \pm 0.2 \, \text{g m}^{-3}$ and $2.2 \pm 0.2 \, \text{g m}^{-3}$ to represent dry and wet growth conditions and to simulate mixed-phase cloud conditions. The wind speed ($3 \, \text{m s}^{-1}$) was chosen to match the typical fall velocity of graupel. The temperature and pH dependences (pH 4 and 5.6) of the compounds were studied as well as the dependence on the growth regimes. Two different rime collectors were also considered, a Teflon-coated metal bar and a graupel. Stuart and Jacobson (2004; 2003) hypothesized a dependence on external influences such as temperature and pH for compounds with a low dimensionless effective Henry's law constant H^*. Of the compounds investigated, 2-nitrophenol has the lowest H^*. In agreement with the current literature, the determined retention coefficients of 2-nitrophenol show a significant dependence on pH and on the type of rime collector. The mean retention coefficients for the graupel samples are $R_{\text{G5.6}} = 0.19 \pm 0.05$ (pH 5.6) and $R_{\text{G4}} = 0.08 \pm 0.04$ (pH 4). This indicates that changes in the pH value can influence retention and must be taken into account. At pH 4 2-nitrophenol also showed a dependence between dry and wet growth conditions. The temperature dependence and the dependence on growth conditions seem to overlap, as the growth conditions differ not only in liquid water content but also in temperature. Since the measured values between dry and wet growth overlap within the experimental uncertainty, a temperature dependence is reported in this study. The higher scattering of the values obtained from the measurements with pH 5.6 could be the reason why the temperature trend and the difference between the growth regimes found at pH 4 are not visible at pH 5.6.

2-Nitrobenzoic acid, 4-nitrophenol, and 4-nitrocatechol showed retention coefficients of 0.99 ± 0.04, 1.01 ± 0.07, and 1.01 ± 0.14, respectively, with no significant dependence on temperature, pH, type of rime collector or growth-regime. For

cis-pinic acid and cis-pinonic acid, retention coefficients of 0.96 ± 0.07 and 0.92 ± 0.11 were obtained, which also showed no dependence on the parameters investigated. This study shows that there appears to be no difference between dry and wet growth conditions for compounds with a high effective Henry's law constant and that H^* can also be used to estimate retention coefficients for wet growth conditions, at least for graupel and the ambient conditions used in this study (wet growth conditions: ambient temperature: -3 and -5 °C; LWC: 2.2 g m^{-3}; surface temperature: -0.8 and -2.2 °C; no shedding of water). This is in contrast to a modelling study by Michael and Stuart (2009), which indicates a lower influence of H^* and low retention coefficients even for compounds with high H^* under wet growth conditions for hailstones. However, it should be noted that in this study, hail was investigated at a surface temperature of 0°C and a shedding of water. It is therefore possible that the differences in the experimental conditions are responsible for the discrepancies in the observed outcomes. The retention coefficient for pinanediol was determined to be 0.98 ± 0.08 with no significant temperature dependence. This would not have been expected due to the comparably low H^*. However, the Henry's law constant is only predicted and may be subject to errors due to the specific structure of the molecule. For this reason, it is important to determine Henry's law constants of more different molecules to aid in the understanding and modeling of processes in the atmosphere.

The retention coefficients for 4-nitrophenol and 2-nitrophenol differ considerably. Since they are structural isomers, it is obvious that they have the same molecular formula and the same functional groups, although they are arranged differently. The different arrangement allows for the formation of an intramolecular hydrogen bond between the OH and the nitro group in 2-nitrophenol. This can result in the non-dissociated form being stabilized, which may explain why 4-nitrophenol exhibits greater solubility than 2-nitrophenol. This could be due to the fact that 4-nitrophenol undergoes easier solvation and displays the capacity to form intermolecular hydrogen bonds. This property may also be responsible for the observed differences in Henry's law constants and retention (Achard et al., 1996; Schwarzenbach et al., 1988). In contrast to the bond method used in this study, the group method of the HENRYWIN^{TM} software predicts the same Henry's law constant for both isomers. This clearly shows the importance of reliable prediction or measurement of H^* and the importance of chemical structure.

It is demonstrated here that the retention coefficients of more complex organic molecules depend mainly on the dimensionless effective Henry's law constant. These experiments have improved the parameterization of retention coefficients using the dimensionless effective Henry's law constant. The results show that the retention of compounds with an H^* below 10^3 is not a significant factor and thus the most of the compound dissolved in the supercooled drops is released into the gas phase during freezing. For compounds with an H^* value above 10^8, a retention close to 1 is expected and the compound remains completely in the ice phase during freezing. These compounds can be effectively washed out by precipitation or transported further upwards and released by sublimation of the ice particles. At high altitudes and low temperatures, the volatility of these compounds is even lower, and it is possible that particulate residuals form after sublimation. This probably has an impact on the chemistry of the upper troposphere and ultimately on the Earth's radiative budget. In the intermediate range of H^*, the improved fit of R vs H^* (Eq. (4), with $a_{\text{red}} = (3.34 \pm 1.61) \cdot 10^4$ and $b_{\text{red}} = 0.36 \pm 0.06$) can be used to estimate the retention coefficient and thus further improve cloud models that account for transport of organic trace components. However,

465   the present results show that more retention measurements are needed for compounds with $10^4 < H^* < 10^6$ to clarify the sharpness of the transition between the two boundaries of zero retention and full retention.

Author contribution

CB, JS, MG, KD, YM, AA, LG, AT, AV, TH designed and performed the wind tunnel experiments; FU synthesized pinic

470   acid; CB performed the analytical measurement, analyzed the data and wrote the manuscript draft; JS, MG, MS; AT; AV; TH reviewed and edited the manuscript.

Competing interests

The authors declare that they have no conflict of interest.

475

References

Achard, C., Jaoui, M., Schwing, M., and Rogalski, M.: Aqueous Solubilities of Phenol Derivatives by Conductivity

480   Measurements, J. Chem. Eng. Data, 41, 504–507, https://doi.org/10.1021/je950202o, 1996.

Andreae, M. O., Afchine, A., Albrecht, R., Holanda, B. A., Artaxo, P., Barbosa, H. M. J., Borrmann, S., Cecchini, M. A., Costa, A., Dollner, M., Fütterer, D., Järvinen, E., Jurkat, T., Klimach, T., Konemann, T., Knote, C., Krämer, M., Krisna, T., Machado, L. A. T., Mertes, S., Minikin, A., Pöhlker, C., Pöhlker, M. L., Pöschl, U., Rosenfeld, D., Sauer, D., Schlager, H., Schnaiter, M., Schneider, J., Schulz, C., Spanu, A., Sperling, V. B., Voigt, C., Walser, A., Wang, J., Weinzierl, B.,

485   Wendisch, M., and Ziereis, H.: Aerosol characteristics and particle production in the upper troposphere over the Amazon Basin, Atmos. Chem. Phys., 18, 921–961, https://doi.org/10.5194/acp-18-921-2018, 2018.

Bardakov, R., Thornton, J. A., Riipinen, I., Krejci, R., and Ekman, A. M. L.: Transport and chemistry of isoprene and its oxidation products in deep convective clouds, Tellus B: Chemical and Physical Meteorology, 73, 1979856, https://doi.org/10.1080/16000889.2021.1979856, 2022.

490   Barth, M. C., Bela, M. M., Fried, A., Wennberg, P. O., Crounse, J. D., St. Clair, J. M., Blake, N. J., Blake, D. R., Homeyer, C. R., Brune, W. H., Zhang, L., Mao, J., Ren, X., Ryerson, T. B., Pollack, I. B., Peischl, J., Cohen, R. C., Nault, B. A., Huey, L. G., Liu, X., and Cantrell, C. A.: Convective transport and scavenging of peroxides by thunderstorms observed over the central U.S. during DC3, Journal of Geophysical Research: Atmospheres, 121, 4272–4295, https://doi.org/10.1002/2015JD024570, 2016.

495   Barth, M. C., Kim, S.-W., Wang, C., Pickering, K. E., Ott, L. E., Stenchikov, G., Leriche, M., Cautenet, S., Pinty, J.-P., Barthe, C., Mari, C., Helsdon, J. H., Farley, R. D., Fridlind, A. M., Ackerman, A. S., Spiridonov, V., and Telenta, B.: Cloud-scale

model intercomparison of chemical constituent transport in deep convection, Atmos. Chem. Phys., 7, 4709–4731, https://doi.org/10.5194/acp-7-4709-2007, 2007a.

Barth, M. C., Kim, S.-W., Skamarock, W. C., Stuart, A. L., Pickering, K. E., and Ott, L. E.: Simulations of the redistribution of formaldehyde, formic acid, and peroxides in the 10 July 1996 Stratospheric-Tropospheric Experiment: Radiation, Aerosols, and Ozone deep convection storm, J. Geophys. Res., 112, https://doi.org/10.1029/2006JD008046, 2007b.

Bela, M. M., Barth, M. C., Toon, O. B., Fried, A., Ziegler, C., Cummings, K. A., Li, Y., Pickering, K. E., Homeyer, C. R., Morrison, H., Yang, Q., Mecikalski, R. M., Carey, L., Biggerstaff, M. I., Betten, D. P., and Alford, A. A.: Effects of Scavenging, Entrainment, and Aqueous Chemistry on Peroxides and Formaldehyde in Deep Convective Outflow Over the Central and Southeast United States, J. Geophys. Res. Atmos., 123, 7594–7614, https://doi.org/10.1029/2018jd028271, 2018.

Bianchi, F., Kurtén, T., Riva, M., Mohr, C., Rissanen, M. P., Roldin, P., Berndt, T., Crounse, J. D., Wennberg, P. O., Mentel, T. F., Wildt, J., Junninen, H., Jokinen, T., Kulmala, M., Worsnop, D. R., Thornton, J. A., Donahue, N., Kjaergaard, H. G., and Ehn, M.: Highly Oxygenated Organic Molecules (HOM) from Gas-Phase Autoxidation Involving Peroxy Radicals: A Key Contributor to Atmospheric Aerosol, Chemical reviews, 119, 3472–3509, https://doi.org/10.1021/acs.chemrev.8b00395, 2019.

Claeys, M., Graham, B., Vas, G., Wang, W., Vermeylen, R., Pashynska, V., Cafmeyer, J., Guyon, P., Andreae, M. O., Artaxo, P., and Maenhaut, W.: Formation of secondary organic aerosols through photooxidation of isoprene, Science (New York, N.Y.), 303, 1173–1176, https://doi.org/10.1126/science.1092805, 2004.

Clarke, A. D., Varner, J. L., Eisele, F., Mauldin R. L., Tanner, D., and Litchy, M.: Particle production in the remote marine atmosphere: Cloud outflow and subsidence during ACE 1, J. Geophys. Res., 103, 16397–16409, 1998.

Cuchiara, G. C., Fried, A., Barth, M. C., Bela, M. M., Homeyer, C. R., Walega, J., Weibring, P., Richter, D., Woods, S., Beyersdorf, A., Bui, T. V., and Dean-Day, J.: Effect of Marine and Land Convection on Wet Scavenging of Ozone Precursors Observed During a SEAC 4 RS Case Study, J. Geophys. Res. Atmos., 128, https://doi.org/10.1029/2022JD037107, 2023.

Desyaterik, Y., Sun, Y., Shen, X., Lee, T., Wang, X., Wang, T., and Collett, J. L.: Speciation of "brown" carbon in cloud water impacted by agricultural biomass burning in eastern China, J. Geophys. Res. Atmos., 118, 7389–7399, https://doi.org/10.1002/jgrd.50561, 2013.

Diehl, K., Mitra, S. K., Szakáll, M., Blohn, N. von, Borrmann, S., and Pruppacher, H. R.: The Mainz vertical wind tunnel facility: a review of 25 years of laboratory experiments on cloud physics and chemistry: Aerodynamics, models, and experiments, Wind Tunnels: Aerodynamics, Models, and Experiments, Nova Science Publisher's, New York, 69-92, 2011.

Fugal, J. P., Schulz, T. J., and Shaw, R. A.: Practical methods for automated reconstruction and characterization of particles in digital in-line holograms, Meas. Sci. Technol., 20, 75501, https://doi.org/10.1088/0957-0233/20/7/075501, 2009.

Fugal, J. P., Shaw, R. A., Saw, E. W., and Sergeyev, A. V.: Airborne digital holographic system for cloud particle measurements, Applied optics, 43, 5987–5995, https://doi.org/10.1364/ao.43.005987, 2004.

Ganranoo, L., Mishra, S. K., Azad, A. K., Shigihara, A., Dasgupta, P. K., Breitbach, Z. S., Armstrong, D. W., Grudpan, K., and Rappenglueck, B.: Measurement of nitrophenols in rain and air by two-dimensional liquid chromatography-chemically active liquid core waveguide spectrometry, Analytical chemistry, 82, 5838–5843, https://doi.org/10.1021/ac101015y, 2010.

535   Gouw, J. de and Jimenez, J. L.: Organic aerosols in the Earth's atmosphere, Environ. Sci. Technol., 43, 7614–7618, https://doi.org/10.1021/es9006004, 2009.

Harrison, M. A., Barra, S., Borghesi, D., Vione, D., Arsene, C., and Iulian Olariu, R.: Nitrated phenols in the atmosphere: a review, Atmospheric Environment, 39, 231–248, https://doi.org/10.1016/j.atmosenv.2004.09.044, 2005.

Haynes, W. M.: CRC Handbook of Chemistry and Physics, CRC Press, 2014.

540   Hine, J. and Mookerjee, P. K.: Structural effects on rates and equilibriums. XIX. Intrinsic hydrophilic character of organic compounds. Correlations in terms of structural contributions, The Journal of Organic Chemistry, 3, 292–298, available at: https://doi.org/10.1021/jo00891a006, 1975.

Hoffmann, T., Odum, J. R., Bowman, F., Collins, D., Klockow, D., Flagan, R. C., and Seinfeld, J. H.: Formation of Organic Aerosols from the Oxidation of Biogenic Hydrocarbons, J Atmos Chem, 26, 189–222,
545   https://doi.org/10.1023/A:1005734301837, 1997.

Iribarne, J. V. and Pyshnov, T.: The effect of freezing on the composition of supercooled droplets—I. Retention of HCl, HNO3, NH3 and H2O2, Atmospheric Environment. Part A. General Topics, 24, 383–387, https://doi.org/10.1016/0960-1686(90)90118-7, 1990.

Jost, A.: Bereifungsexperimente zur Bestimmung des SO2 - Retentionskoeffizienten; durchgeführt am vertikalen Windkanal
550   der Johannes Gutenberg Universität Mainz, Diplomarbeit, Institut für Physik der Atmosphäre, Johannes Gutenberg Universität Mainz, Mainz, 189 pp., 2012.

Jost, A., Szakáll, M., Diehl, K., Mitra, S. K., and Borrmann, S.: Chemistry of riming: the retention of organic and inorganic atmospheric trace constituents, Atmos. Chem. Phys., 17, 9717–9732, https://doi.org/10.5194/acp-17-9717-2017, 2017.

Kerminen, V.-M., Chen, X., Vakkari, V., Petäjä, T., Kulmala, M., and Bianchi, F.: Atmospheric new particle formation and
555   growth: review of field observations, Environ. Res. Lett., 13, 103003, https://doi.org/10.1088/1748-9326/aadf3c, 2018.

Kołodziejczyk, A., Pyrcz, P., Błaziak, K., Pobudkowska, A., Sarang, K., and Szmigielski, R.: Physicochemical Properties of Terebic Acid, MBTCA, Diaterpenylic Acid Acetate, and Pinanediol as Relevant α-Pinene Oxidation Products, ACS omega, 5, 7919–7927, https://doi.org/10.1021/acsomega.9b04231, 2020.

Kołodziejczyk, A., Pyrcz, P., Pobudkowska, A., Błaziak, K., and Szmigielski, R.: Physicochemical Properties of Pinic,
560   Pinonic, Norpinic, and Norpinonic Acids as Relevant α-Pinene Oxidation Products, The journal of physical chemistry. B, 123, 8261–8267, https://doi.org/10.1021/acs.jpcb.9b05211, 2019.

Kroll, J. H. and Seinfeld, J. H.: Chemistry of secondary organic aerosol: Formation and evolution of low-volatility organics in the atmosphere, Atmospheric Environment, 42, 3593–3624, https://doi.org/10.1016/j.atmosenv.2008.01.003, 2008.

List, R.: Zur Thermodynamik teilweise wässriger Hagelkörner, Journal of Applied Mathematics and Physics (ZAMP), 11, 273–306, https://doi.org/10.1007/BF01602676, 1960.

Löflund, M., Kasper-Giebl, A., Schuster, B., Giebl, H., Hitzenberger, R., and Puxbaum, H.: Formic, acetic, oxalic, malonic and succinic acid concentrations and their contribution to organic carbon in cloud water, Atmospheric Environment, 36, 1553–1558, https://doi.org/10.1016/S1352-2310(01)00573-8, 2002.

Lohmann, U., Lüönd, F., and Mahrt, F.: An introduction to clouds: From the microscale to climate, First published 2016. Reprinted 2020, Cambridge University Press, Cambridge, XXVI, 391 stron, [16] stron tablic, 2020.

Macklin, W. C.: Accretion in mixed clouds, Quart J Royal Meteoro Soc, 87, 413–424, https://doi.org/10.1002/qj.49708737312, 1961.

Meylan, W. M. and Howard, P. H.: Bond contribution method for estimating henry's law constants, Environmental Toxicology and Chemistry, 10, 1283–1293, available at: https://doi.org/10.1002/etc.5620101007, 1991.

Michael, R. and Stuart, A. L.: The fate of volatile chemicals during wet growth of a hailstone, Environ. Res. Lett., 4, 15001, https://doi.org/10.1088/1748-9326/4/1/015001, 2009.

Müller, L., Reinnig, M.-C., Naumann, K. H., Saathoff, H., Mentel, T. F., Donahue, N. M., and Hoffmann, T.: Formation of 3-methyl-1,2,3-butanetricarboxylic acid via gas phase oxidation of pinonic acid – a mass spectrometric study of SOA aging, Atmos. Chem. Phys., 12, 1483–1496, https://doi.org/10.5194/acp-12-1483-2012, 2012.

Nozière, B., Kalberer, M., Claeys, M., Allan, J., D'Anna, B., Decesari, S., Finessi, E., Glasius, M., Grgić, I., Hamilton, J. F., Hoffmann, T., Iinuma, Y., Jaoui, M., Kahnt, A., Kampf, C. J., Kourtchev, I., Maenhaut, W., Marsden, N., Saarikoski, S., Schnelle-Kreis, J., Surratt, J. D., Szidat, S., Szmigielski, R., and Wisthaler, A.: The molecular identification of organic compounds in the atmosphere: state of the art and challenges, Chemical reviews, 115, 3919–3983, https://doi.org/10.1021/cr5003485, 2015.

Pflaum, J. C. and Pruppacher, H. R.: A Wind Tunnel Investigation of the Growth of Graupel Initiated from Frozen Drops, J. Atmos. Sci., 36, 680–689, https://doi.org/10.1175/1520-0469(1979)036<0680:AWTIOT>2.0.CO;2, 1979.

Pruppacher, H. R. and Klett, J. D.: Microphysics of Clouds and Precipitation, 18, Springer Netherlands, Dordrecht, 975 pp., 2010.

Pye, H. O. T., Nenes, A., Alexander, B., Ault, A. P., Barth, M. C., Clegg, S. L., Collett, J. L., Fahey, K. M., Hennigan, C. J., Herrmann, H., Kanakidou, M., Kelly, J. T., Ku, I.-T., McNeill, V. F., Riemer, N., Schaefer, T., Shi, G., Tilgner, A., Walker, J. T., Wang, T., Weber, R., Xing, J., Zaveri, R. A., and Zuend, A.: The Acidity of Atmospheric Particles and Clouds, Atmospheric chemistry and physics, 20, 4809–4888, https://doi.org/10.5194/acp-20-4809-2020, 2020.

Reijenga, J., van Hoof, A., van Loon, A., and Teunissen, B.: Development of Methods for the Determination of pKa Values, Analytical chemistry insights, 8, 53–71, https://doi.org/10.4137/ACI.S12304, 2013.

Schwarzenbach, R. P., Stierli, R., Folsom, B. R., and Zeyer, J.: Compound properties relevant for assessing the environmental partitioning of nitrophenols, Environ. Sci. Technol., 22, 83–92, https://doi.org/10.1021/es00166a009, 1988.

Simon, M., Dada, L., Heinritzi, M., Scholz, W., Stolzenburg, D., Fischer, L., Wagner, A. C., Kürten, A., Rörup, B., He, X.-C., Almeida, J., Baalbaki, R., Baccarini, A., Bauer, P. S., Beck, L., Bergen, A., Bianchi, F., Bräkling, S., Brilke, S., Caudillo, L., Chen, D., Chu, B., Dias, A., Draper, D. C., Duplissy, J., El-Haddad, I., Finkenzeller, H., Frege, C., Gonzalez-Carracedo, L., Gordon, H., Granzin, M., Hakala, J., Hofbauer, V., Hoyle, C. R., Kim, C., Kong, W., Lamkaddam, H., Lee, C. P., Lehtipalo, K., Leiminger, M., Mai, H., Manninen, H. E., Marie, G., Marten, R., Mentler, B., Molteni, U., Nichman, L., Nie, W., Ojdanic, A., Onnela, A., Partoll, E., Petäjä, T., Pfeifer, J., Philippov, M., Quéléver, L. L. J., Ranjithkumar, A., Rissanen, M. P., Schallhart, S., Schobesberger, S., Schuchmann, S., Shen, J., Sipilä, M., Steiner, G., Stozhkov, Y., Tauber, C., Tham, Y. J., Tomé, A. R., Vazquez-Pufleau, M., Vogel, A. L., Wagner, R., Wang, M., Wang, D. S., Wang, Y., Weber, S. K., Wu, Y., Xiao, M., Yan, C., Ye, P., Ye, Q., Zauner-Wieczorek, M., Zhou, X., Baltensperger, U., Dommen, J., Flagan, R. C., Hansel, A., Kulmala, M., Volkamer, R., Winkler, P. M., Worsnop, D. R., Donahue, N. M., Kirkby, J., and Curtius, J.: Molecular understanding of new-particle formation from α-pinene between −50 and +25 °C, Atmos. Chem. Phys., 20, 9183–9207, https://doi.org/10.5194/acp-20-9183-2020, 2020.

Sindelarova, K., Granier, C., Bouarar, I., Guenther, A., Tilmes, S., Stavrakou, T., Müller, J.-F., Kuhn, U., Stefani, P., and Knorr, W.: Global data set of biogenic VOC emissions calculated by the MEGAN model over the last 30 years, Atmos. Chem. Phys., 14, 9317–9341, https://doi.org/10.5194/acp-14-9317-2014, 2014.

Snider, J. R. and Huang, J.: Factors influencing the retention of hydrogen peroxide and molecular oxygen in rime ice, J. Geophys. Res., 103, 1405–1415, https://doi.org/10.1029/97JD02847, 1998.

Snider, J. R., Montague, D. C., and Vali, G.: Hydrogen peroxide retention in rime ice, J. Geophys. Res., 97, 7569–7578, https://doi.org/10.1029/92JD00237, 1992.

Spolnik, G., Wach, P., Rudziński, K. J., Szmigielski, R., and Danikiewicz, W.: Tracing the biogenic secondary organic aerosol markers in rain, snow and hail, Chemosphere, 251, 126439, https://doi.org/10.1016/j.chemosphere.2020.126439, 2020.

Stolzenburg, D., Fischer, L., Vogel, A. L., Heinritzi, M., Schervish, M., Simon, M., Wagner, A. C., Dada, L., Ahonen, L. R., Amorim, A., Baccarini, A., Bauer, P. S., Baumgartner, B., Bergen, A., Bianchi, F., Breitenlechner, M., Brilke, S., Buenrostro Mazon, S., Chen, D., Dias, A., Draper, D. C., Duplissy, J., El Haddad, I., Finkenzeller, H., Frege, C., Fuchs, C., Garmash, O., Gordon, H., He, X., Helm, J., Hofbauer, V., Hoyle, C. R., Kim, C., Kirkby, J., Kontkanen, J., Kürten, A., Lampilahti, J., Lawler, M., Lehtipalo, K., Leiminger, M., Mai, H., Mathot, S., Mentler, B., Molteni, U., Nie, W., Nieminen, T., Nowak, J. B., Ojdanic, A., Onnela, A., Passananti, M., Petäjä, T., Quéléver, L. L. J., Rissanen, M. P., Sarnela, N., Schallhart, S., Tauber, C., Tomé, A., Wagner, R., Wang, M., Weitz, L., Wimmer, D., Xiao, M., Yan, C., Ye, P., Zha, Q., Baltensperger, U., Curtius, J., Dommen, J., Flagan, R. C., Kulmala, M., Smith, J. N., Worsnop, D. R., Hansel, A., Donahue, N. M., and Winkler, P. M.: Rapid growth of organic aerosol nanoparticles over a wide tropospheric temperature range, Proceedings of the National Academy of Sciences of the United States of America, 115, 9122–9127, https://doi.org/10.1073/pnas.1807604115, 2018.

Stuart, A. L. and Jacobson, M. Z.: Chemical retention during dry growth riming, J. Geophys. Res., 109, https://doi.org/10.1029/2003JD004197, available at: https://doi.org/10.1029/2003JD004197, 2004.

Stuart, A. L. and Jacobson, M. Z.: A timescale investigation of volatile chemical retention during hydrometeor freezing: Nonrime freezing and dry growth riming without spreading, J. Geophys. Res., 108, https://doi.org/10.1029/2001JD001408, 2003.

Szakáll, M., Mitra, S. K., Diehl, K., and Borrmann, S.: Shapes and oscillations of falling raindrops — A review, Atmospheric Research, 97, 416–425, https://doi.org/10.1016/j.atmosres.2010.03.024, 2010.

Theis, A., Szakáll, M., Diehl, K., Mitra, S. K., Zanger, F., Heymsfield, A., and Borrmann, S.: Vertical Wind Tunnel Experiments and a Theoretical Study on the Microphysics of Melting Low-Density Graupel, J. Atmos. Sci., 79, 1069–1087, https://doi.org/10.1175/JAS-D-21-0162.1, 2022.

Twohy, C. H., Clement, C. F., Gandrud, B. W., Weinheimer, A. J., Campos, T. L., Baumgardner, D., Brune, W. H., Faloona, I., Sachse, G. W., Vay, S. A., and Tan, D.: Deep convection as a source of new particles in the midlatitude upper troposphere, J. Geophys. Res., 107, https://doi.org/10.1029/2001JD000323, 2002.

US EPA.: Estimation Programs Interface Suite™ for Microsoft® Windows, v 4.1, United States Environmental Protection Agency, Washington, DC, USA, 2012.

v. Blohn, N., Diehl, K., Nölscher, A., Jost, A., Mitra, S. K., and Borrmann, S.: The retention of ammonia and sulfur dioxide during riming of ice particles and dendritic snow flakes: laboratory experiments in the Mainz vertical wind tunnel, J Atmos Chem, 70, 131–150, https://doi.org/10.1007/s10874-013-9261-x, 2013.

v. Blohn, N., Diehl, K., Mitra, S. K., and Borrmann, S.: Wind tunnel experiments on the retention of trace gases during riming: nitric acid, hydrochloric acid, and hydrogen peroxide, Atmos. Chem. Phys., 11, 11569–11579, https://doi.org/10.5194/acpd-11-17447-2011, 2011.

v. Blohn, N., Diehl, K., Mitra, S. K., and Borrmann, S.: Riming of Graupel: Wind Tunnel Investigations of Collection Kernels and Growth Regimes, J. Atmos. Sci., 66, 2359–2366, https://doi.org/10.1175/2009JAS2969.1, 2009.

Wang, H., Gao, Y., Wang, S., Wu, X., Liu, Y., Li, X., Huang, D., Lou, S., Wu, Z., Guo, S., Jing, S., Li, Y., Huang, C., Tyndall, G. S., Orlando, J. J., and Zhang, X.: Atmospheric Processing of Nitrophenols and Nitrocresols From Biomass Burning Emissions, J. Geophys. Res. Atmos., 125, https://doi.org/10.1029/2020JD033401, 2020.

Wang, P. K. and Kubicek, A.: Flow fields of graupel falling in air, Atmospheric Research, 124, 158–169, https://doi.org/10.1016/j.atmosres.2013.01.003, 2013.

Weitzel, M., Mitra, S. K., Szakáll, M., Fugal, J. P., and Borrmann, S.: Application of holography and automated image processing for laboratory experiments on mass and fall speed of small cloud ice crystals, Atmos. Chem. Phys., 20, 14889–14901, https://doi.org/10.5194/acp-20-14889-2020, 2020.

Williamson, C. J., Kupc, A., Axisa, D., Bilsback, K. R., Bui, T., Campuzano-Jost, P., Dollner, M., Froyd, K. D., Hodshire, A. L., Jimenez, J. L., Kodros, J. K., Luo, G., Murphy, D. M., Nault, B. A., Ray, E. A., Weinzierl, B., Wilson, J. C., Yu, F., Yu, P., Pierce, J. R., and Brock, C. A.: A large source of cloud condensation nuclei from new particle formation in the tropics, Nature, 574, 399–403, https://doi.org/10.1038/s41586-019-1638-9, 2019.

Xiao, Q., Zhang, J., Wang, Y., Ziemba, L. D., Crosbie, E., Winstead, E. L., Robinson, C. E., DiGangi, J. P., Diskin, G. S.,
665   Reid, J. S., Schmidt, K. S., Sorooshian, A., Hilario, M. R. A., Woods, S., Lawson, P., Stamnes, S. A., and Wang, J.: New
        particle formation in the tropical free troposphere during CAMP 2 Ex: statistics and impact of emission sources, convective
        activity, and synoptic conditions, Atmos. Chem. Phys., 23, 9853–9871, https://doi.org/10.5194/acp-23-9853-2023, 2023.